Fachtagung "Experimentelle Strömungsmechanik"
3.-5. September 2019, Erlangen

Heat transfer in deformable foams by the means of multicomponent Lattice Boltzmann Method

Mohammad Mobarak, Bernhard Gatternig, Mohamed Hussein, Anuhar Osorio, Antonio Delgado.
Lehrstuhl für Strömungsmechanik
Friedrich-Alexander-Universität Erlangen-Nürnberg
Cauerstraße 4
91058 Erlangen

Lattice Boltzmann Method, Multiphase-Multicomponent flow, Shan-Chen Pseudopotential Model, Thermal Flows, Food Foams.

Abstract

Foam propagation is a complex and challenging topic in food and chemical industry. Foam exists in several industrial applications such as food supply and discharge pipes, dairy products tanks and rectification columns. Foams often influence the mass, momentum and energy transport as well as the biochemical reactions. Consequently, this leads to a significant additional consumption of time and energy, and also to a loss of product quality and safety.
The proposed approach is to apply a multi-component Lattice Boltzmann method, namely Shan-Chen pseudopotential model coupled with thermal LBM in order to simulate the complex heat transfer process in foams, taking into account the foam dynamics and deformation. The approach is to use multi-distribution functions for the multicomponent flow and temperature fields considering the different physical parameters for each phenomenon.
The Lattice Boltzmann Method (LBM) has recently gained great attention in thermal flow field modelling, especially in complex media. One great advantage of the method is that it handles complex geometries and obstacles in a simple manner. LBM also gained much attention and success in the field of multicomponent and multiphase flows, one benefit is that it does not need an explicit additional algorithm for interface tracking.
These simulations will provide a deeper insight in the foam dynamics and heat transfer process inside this nonhomogeneous medium. This can provide the basis for a prediction tool that regards the foaming causes and effects in several industrial processes. Several Industrial sectors with various products like beverages and milk can benefit from this tool, as the foaming in beverages' filling and dairy production can be controlled and optimized on this basis. Other applications are chemical production facilities that deal with columns and evaporators which also encounter critical foaming issues.

Introduction

The Lattice Boltzmann Method (LBM) has recently gained much attention in the field of fluid mechanics, including multi-phase, thermal, complex and micro-scale media flows with high Knudsen number, at scales where continuum assumption fails. LBM is a hyper stylized version of the Boltzmann equation explicitly designed to solve fluid-dynamics problems, and beyond, see Succi 2001. The main interest through this work is to implement LBM accordingly with the Shan-Chen pseudopotential model (X. Shan and H. Chen 1993) in order to model bubble flow in liquids. The approach is to use both interaction forces for the multiphase and the multicomponent parts in order to reach a higher density ratio compared to solely using the multicomponent part (L. Chen et al. 2014). This is done by two distribution functions responsible for each component, while the higher density component is kept in the liquid phase. The model is also complemented by a one-way-coupled temperature field using a third distribution function where thermal flow is considered during conduction and convection by the solved multiphase

GALA e.V., Karlsruhe, Germany, ISBN 978-3-9816764-6-4

multicomponent flow field. The built model is applied to a bubble rising in a rectification column where the bubbles are initiated with the boiling temperature of the liquid during evaporation. Although this model considers both thermal and the multiphase physics, the temperature effect on the equation of state and thus the dependency of the liquid-gas coexistence on temperature is not yet considered. Different LBM forcing schemes (Guo et al. 2002, Buick and Greated 2000) and equations of state (P. Yuan et al. 2006) have been numerically investigated in order to reach the aimed goal.

Lattice Boltzmann Method

The Lattice Boltzmann Method can be considered as a finite difference scheme of the classical Ludwig Boltzmann's Equation (BE) "equation (1)" – which models the particles interactions through the particle distribution function f – in the discretised form, see Chen, S. and Doolen, G.D., 1998, in accordance with the Bhatnagar-Gross Krook (BGK) approximation – namely single relaxation time (SRT) – for the collision operator Q, see Koelman 1991, where v is the particle velocity.

$$\frac{\partial f}{\partial t} + v \cdot \nabla f = Q \tag{1}$$

Then, the collision operator Q can be expressed as follows:

$$Q_i = -\frac{1}{\tau}\left[f_i - f_i^{(equ)} \right] \tag{2}$$

where $f_i^{(equ)}$ is the local equilibrium distribution function evaluated from the Maxwell-Boltzmann distribution and τ is the relaxation time for the particles to move from the non-equilibrium to the equilibrium state during collision. The LBE which carries the core procedure of the method can be expressed as:

$$f_i(x + \hat{e}_i \Delta t, t + \Delta t) = f_i(x,t) - \frac{1}{\tau}\left(f_i(x,t) - f_i^{equ}(x,t) \right) \tag{3}$$

The equilibrium distribution function truncated at the second order velocity term evaluated from the Hermite expansion of the Maxwellian distribution function – which satisfies the dynamic collision invariants; number, momentum, particle kinetic energy, see Hussein 2010 – can be expressed as:

$$f_i^{equ} = w_i \rho \left[1 + 3\frac{\hat{e}_i \cdot \hat{u}}{c^2} + \frac{9}{2}\frac{(\hat{e}_i \cdot \hat{u})^2}{c^4} - \frac{3}{2}\frac{\hat{u} \cdot \hat{u}}{c^2} \right] \tag{4}$$

where $\hat{e}_i$, w_i, c and u are the discrete unit vectors, the weighting parameter, the lattice speed $c = \frac{\Delta x}{\Delta t}$ and the macroscopic velocity respectively. The lattice can be either D2Q9 or D3Q19 (Figure 1) & (Table 1)

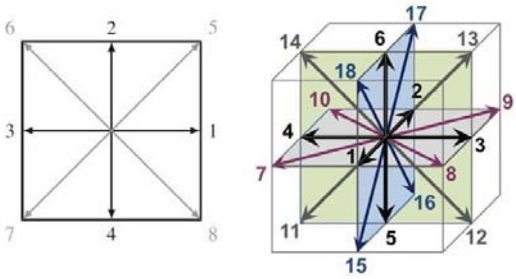

Figure 1: Left: D2Q9 Lattice for two-dimensional representation with 9 particle degrees of freedom, Right: D3Q19 Lattice for three-dimensional representation with 19 particle degrees of freedom (Hussein 2010).

GALA e.V., Karlsruhe, Germany, ISBN 978-3-9816764-6-4

D2Q9		D3Q19	
Direction $\hat{e}_i$	Weighting parameter w_i	Direction $\hat{e}_i$	Weighting parameter w_i
0	4/9	0	1/3
1, 2, 3, 4	1/9	1, 2, 3, 4	1/18
5, 6, 7, 8, 9	1/36	5, 6, 7, 8, 9	1/36

Table 1: Weighting parameters for D2Q9 and D3Q19 lattices.

The macroscopic density and speed are evaluated from the zeroth and the first moment of the distribution function respectively as:

$$\rho = \sum_i f_i \; ; \hat{u} = \frac{1}{\rho} \sum_i f_i \; \hat{e}_i \tag{5}$$

The Mach number and the lattice speed of sound c_s are expressed as:

$$M = \frac{u}{c_s}; \; c_s = \frac{c}{\sqrt{3}} \tag{6}$$

While the pressure is related to the macroscopic density in the incompressible limit through the isothermal gas relation as:

$$P = \rho c_s \tag{7}$$

Now, the relaxation time is evaluated from the fluid kinematic viscosity v from a relation between the Chapman-Enskog expansion of the LBM and the incompressible Navier-Stokes equation, see Succi 2001, which can be written as:

$$\tau \; = 3v + \frac{1}{2} \tag{8}$$

Shan-Chen Pseudopotential Model

The proposed work is based on the multiphase-multicomponent model proposed by X. Shan and H. Chen 1993. The model bases upon presenting the repulsive and attraction forces interacting between components and phases respectively through an external force added to the Lattice Boltzmann Method depending on the associated forcing scheme. The model is based on a certain non-ideal equation of state proposed by Shan-Chen which resembles the Maxwell area construction rule where two phases of fluid are allowed to coexist in the same temperature and pressure. The equation of state for both multiphase multicomponent can be expressed accordingly as:

$$p = {c_s}^2 \sum_{\sigma} \rho^{(\sigma)} + \frac{{c_s}^2}{2} \sum_{\sigma,\tilde{\sigma}} G_{\sigma\tilde{\sigma}} \psi^{(\sigma)} \psi^{(\tilde{\sigma})} \tag{9}$$

where $p, \rho^{(\sigma)}, G_{\sigma\tilde{\sigma}}$ are the static pressure, fluid density of each component and the interaction parameter between phases and components responsible for phase separation and for controlling the fluid surface tension respectively while σ is representing the different components, typically equivalent to 1 and 2 of the different phases.
The model proposes under these conditions two LBE with two distribution functions representing each component of the fluid.

$$f_i^{(\sigma)}(x + \hat{e}_i \Delta t, t + \Delta t) = {f^{(\sigma)}}_i(x,t) - \frac{1}{\tau^{(\sigma)}} \left(f_i^{(\sigma)}(x,t) - {f_i^{equ}}^{(\sigma)}(x,t) \right) \tag{10}$$

GALA e.V., Karlsruhe, Germany, ISBN 978-3-9816764-6-4

where $\tau^{(\sigma)}$ is the relaxation time for each component, representing their different kinematic viscosities. The interacting force incorporated with both the multiphase multicomponent and the pseudopotential function can be written respectively as:

$$\underline{F}_{SC}^{(\sigma)}(x) = -\psi^{(\sigma)}(x)\sum_{\bar{\sigma}} G_{\sigma\bar{\sigma}} \sum_{i} w_i \psi^{(\bar{\sigma})}(x + c_i \Delta t)\underline{e_i} \tag{11}$$

$$\psi^{(\sigma)}(x) = \rho_o \left[1 - e^{\frac{-\rho^{(\sigma)}}{\rho_o}}\right] \tag{12}$$

while ρ_o is traditionally considered as unity. The proposed model can be seen to overtake the Free-energy approach (Swift et al. 1995, 1996) regarding the density ratio, which could only reach density ratios far below our requirements (Krüger et al. 2017). The SC model also overtakes the color method proposed by Gunsten et al. 1991 regarding the interface tracking, In the SC model no explicit interface tracking algorithm is required, the phases are separated automatically following the rules of momentum conservation according to the interaction forces, which is crucial in the complex foam structures. In the color method, the extra collision operator does not cause by itself the phase separation, so the color distribution functions for both components shall be redistributed during simulation in order to maintain the interfaces (Chen, S. and Doolen, G.D., 1998).
Worth to mention that SC approach is not producing a perfectly immiscible fluids i.e. non-zero concentration is still shown in **Fehler! Verweisquelle konnte nicht gefunden werden.**. The fluid will be partially or nearly immiscible depending on the interaction parameter, though traces of the components can be seen in the whole domain, though, reaching a plateau value for higher interaction parameters.

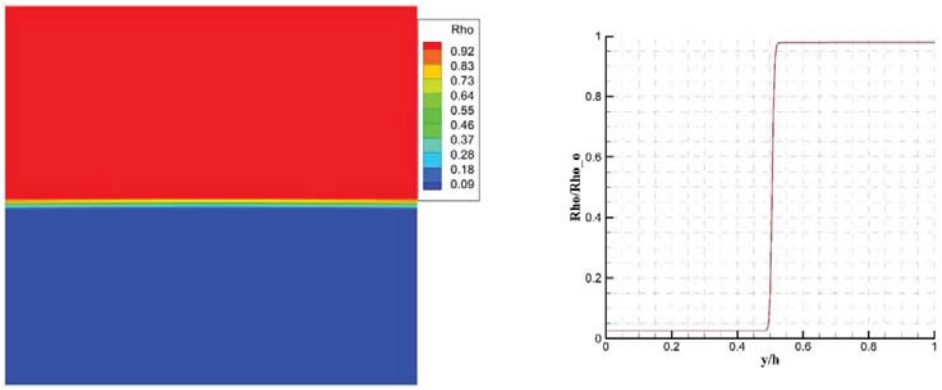

Figure 2: Left: Two component fluid concentration with interface in their steady state. Right: Normalised Density profile across the interface between two immiscible fluids

Forcing Schemes

The model by Shan-Chen shall be accompanied by a forcing scheme, knowing that the basic contribution of this model is defining the isotropic force responsible for the interacting attraction and repulsive forces between phases and components, while the forcing scheme has different approaches and methods. Here, three methods have been investigated, the method by Buick and Greated 2000, the forcing scheme accompanied by Shan-Chen model itself and the approach by Guo et al. 2002. More details about the forcing schemes can be found in the work by Ladd and Verberg 2001. Also, in the work by Guo et al. 2002, the error effect of each forcing scheme on continuity and momentum has been investigated.
It was investigated and alleged by Yu and Fan 2010 that the model by Guo can produce a τ-independent (viscosity independent) surface tension. The forcing scheme by Guo et al. when

GALA e.V., Karlsruhe, Germany, ISBN 978-3-9816764-6-4

numerically investigated gave the least spurious currents near interfaces and hence the highest stable interaction parameter $|G|$, leading to the highest available surface tension and density ratio by the SRT LBM compared to the other two schemes.
The forcing scheme by Guo et al. can be summarized as following; first, the corrected velocity shall be evaluated as:

$$\underline{u}^{*(\sigma)} = \frac{1}{\rho}\left(\sum_i f_i^{(\sigma)} + \frac{F_{SC}{}^{(\sigma)}}{2}\right);\ \rho = \sum_\sigma \rho^{(\sigma)};\ \rho^{(\sigma)} = \sum_i f_i^{(\sigma)} \tag{13}$$

where $\underline{u}^{*(\sigma)}$ is the macroscopic velocity used in the equilibrium distribution function evaluation for each component. Then, the forcing is directly applied after collision to the LBE as a source term $\left(1-\frac{1}{2\tau^{(\sigma)}}\right)F_i^{(\sigma)}$, where this force is evaluated as:

$$F_i^{(\sigma)} = w_i\left(\frac{1}{c_s^{\,2}}F_{SC_\alpha}{}^{(\sigma)}\cdot e_{i\alpha} + \frac{1}{c_s^{\,4}}(e_{i\alpha}e_{i\beta} - \frac{\delta_{\alpha\beta}}{c_s^{\,2}})F_{SC_\alpha}{}^{(\sigma)}u_\beta{}^{*(\sigma)}\right) \tag{14}$$

where $\alpha,\beta = 1,2$ for 2D lattice and $\alpha,\beta = 1,2,3$ for 3D lattice.

Equations of State

Various equations of state have been developed in order to model real gases rather than ideal or perfect gases. One example is the first proposed by van der Waals in 1873, where the deviation from the ideal gas EOS is incorporated by considering the effect of intermolecular attraction forces and the volume occupied by the gas molecules through the two constants a and b which are evaluated from critical temperature and pressure of the pure substance. The vdW EOS is expressed as:

$$p = \frac{\rho RT}{1-b\rho} - a\rho^2 \tag{15}$$

The work proposed by Yuan and Schaefer 2006 was mainly to implement various EOS into the potential function in the SC model “equation (16)”. Leading to a temperature dependent realistic EOS and perhaps reduced the spurious currents, hence higher density ratios.

$$\psi = \sqrt{\frac{2}{G c_s^{\,2}}\left(p - \rho c_s^{\,2}\right)} \tag{16}$$

Another EOS proposed by Carnahan-Starling can be implemented into the potential function which modifies the first term in vdW EOS leading to a more accurate representation of the behavior of real gases.

$$p = \rho RT\frac{1 + b\rho/4 + (b\rho/4)^2 - (b\rho/4)^3}{(1-b\rho/4)^3} - a\rho^2 \tag{17}$$

Both vdW and CS EOS were numerically experimented, though not yet reached the aimed stable high density ratios $\mathcal{O}(1000)$. It is worth to mention that the model stability is very sensitive to the density initialization of fluid phases and components.

Young-Laplace Test

In order to simulate two components in SC model with different densities, one shall initiate two fluids components (low density “1” and high density “2”), while the high-density fluid has to be kept in its liquid phase, and its gas phase will coexist with the other lowdensity component. Now, we have to tune the interaction parameter between both phases in the high density component (G_{22}) and the interaction parameter between the high and low density components ($G_{12} = G_{21}$) in order to reach the required density ratio and surface tension.

GALA e.V., Karlsruhe, Germany, ISBN 978-3-9816764-6-4

For the surface tension, a typical numerical test is performed, which dictates to initialize a bubble with an appropriate pressure. Then, by reaching the steady state of the bubble (Figure 3), one shall calculate the Laplace pressure from the static pressure outside and inside the bubble accordingly with the bubble radius to estimate the equivalent surface tension using the simplified relation for 2D and 3D bubbles:

$$p_{inner} - p_{outer} = \begin{cases} \gamma / R & 2D \\ 2\gamma / R & 3D \end{cases} \tag{18}$$

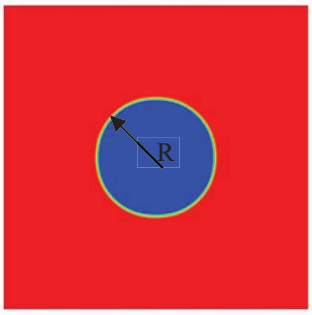

Figure 3: 2D Bubble after reaching the simulation steady state

Thermal LBM

In order to introduce the thermal LBM, one shall use a new distribution function for the temperature field where the LBE will be expressed as follows:

$$T_i(x + \hat{e}_i \Delta t, t + \Delta t) = T_i(x,t) - \frac{1}{\tau_T}\left(T_i(x,t) - T_i^{equ}(x,t)\right) \tag{19}$$

where the equilibrium distribution function for temperature field is evaluated from the macroscopic temperature by the zeroth moment $T = \sum_i T_i$, while the macroscopic velocity is directly implemented and one-way coupled from the multiphase multicompetent flow field as following:

$$T_i^{equ} = w_i T\left[1 + 3\frac{\hat{e}_i \cdot \hat{u}}{c^2} + \frac{9}{2}\frac{(\hat{e}_i \cdot \hat{u})^2}{c^4} - \frac{3}{2}\frac{\hat{u} \cdot \hat{u}}{c^2}\right] \tag{20}$$

Similarly, the relaxation time for the temperature distribution function is related to the thermal diffusivity α based locally on each fluid properties through:

$$\tau_T = 3\alpha + \frac{1}{2} \tag{21}$$

Case Study: Bubbles rising in a rectification column

As an example for applying the above mentioned models and modification recipes, they were implemented in a simulation of bubbles rising in a rectification column. The bubbles were initiated at the bottom resembling the local evaporation that can occur close to the heater. The bubbles were initiated with the boiling temperature of the liquid Tb. The domain is basically 2D with all walls using the no-slip boundary condition for multiphase-multicomponent flow field, while Dirichlet boundary condition was set on the walls for the thermal field as 0.1Tb. The domain was split between the high-density component in liquid phase at the bottom, and gas phase coexisted with the low-density component on top, both initiated at 0.1Tb. The gas bubbles were allowed to rise under gravity with their thermal field, showing the effect of temperature propagation due to conduction and convection. In Figure 4 as for the flow field, the coalescence between bubbles inside the liquid (Scope A) and merging with the low-density component when reaching the liquid surface (Scope B) were clearly shown. Scope C shows the effect of the disturbance occurring from previous bubble's rupture when reaching the interface

GALA e.V., Karlsruhe, Germany, ISBN 978-3-9816764-6-4

which appeared on the deformation of the still existing bubble – near the interface – in the high density component.

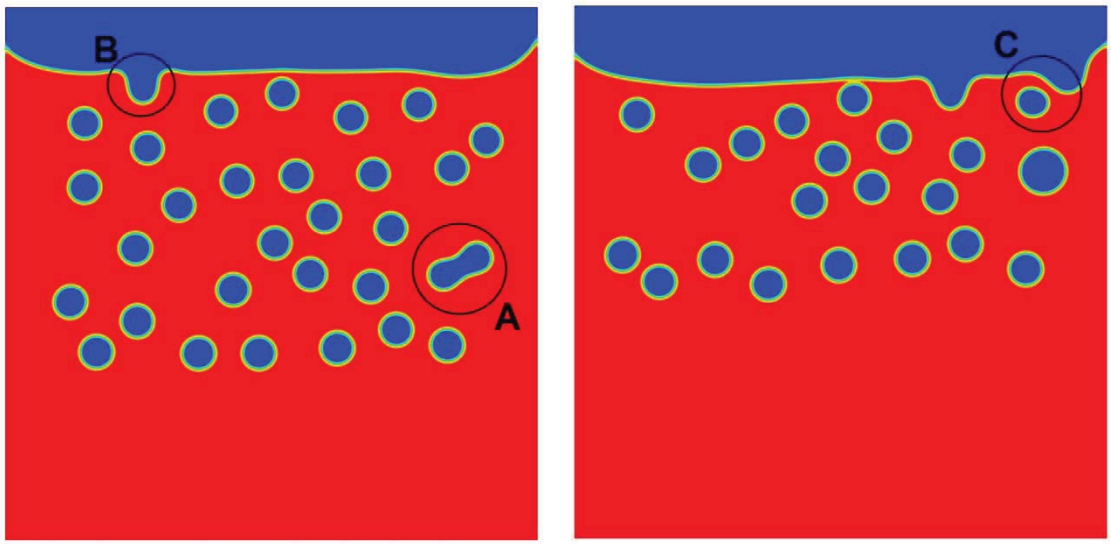

Figure 4: Density field of high-density fluid component (Red: liquid phase, Blue: Gas phase). Scopes A, B & C show the bubble coalescence and deformation. Left and Right are different time stamps.

According to the different thermal diffusivities between the high-density component gas and liquid phases, along with the low density component, the thermal field can be shown as in Figure 5. Traces of high temperature can be shown due to the motion of the bubbles of initially high temperature, while the bubbles themselves are getting colder through their path. At the scope A, two bubbles merged and their two traces are shown, while the new forming bubble is having a slightly lower temperature due to the higher area exposure with the cold liquid phase. Bubbles, when collapsing at the interface, make instantaneous spikes in the temperature field (Scope B), though its effect diminishes by time, since the walls are isothermal and not adiabatic. It is worth to mention that the re-condensation won't be available here in this approach, since, as mentioned before, the multiphase equation of state is still temperature independent, so the temperature field is still one way coupled with the multiphase flow field.

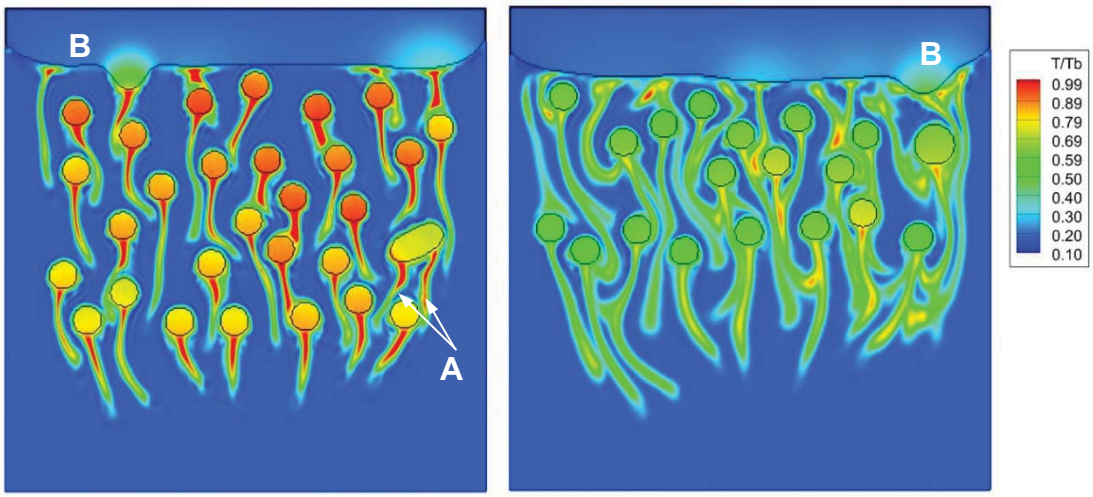

Figure 5: Normalized temperature distribution. Scope A shows the temperature traces from two coalesced bubbles. Scope B shows the disturbance due to bubble rupture at the interface. Left and Right are different time stamps.

GALA e.V., Karlsruhe, Germany, ISBN 978-3-9816764-6-4

Conclusions

The model could capture different physical aspects with very fine details and seems as a promising tool to reach the complete mesoscopic insight for the foaming process, complementary with the macroscopic approach. However, the time scales still need to be adjusted through the non-dimensional groups (Reynolds number, Bond number and Fourier number) which is crucial to simulate the complete physical phenomena with the physical time scales. Reaching a higher, yet stable density ratio from $\mathcal{O}(100)$ to $\mathcal{O}(1000)$ is the challenging future work for this approach. Switching from SRT to MRT (multi relaxation time) is still an option, while deeper investigations on the various equations of state are still required.

Acknowledgement

This work has been supported by the FEI (Forschungskreis der Ernährungsindustrie), AiF (Arbeitsgemeinschaft industrieller Forschungsvereinigungen), and the Ministry of Economics and Technology. This research is part of the DFG/AiF project: " Physikalisch basiertes Management störender Schäume in Produktionsanlagen: Prävention, Inhibierung und Zerstörung".

References

Buick, J.M. and Greated, C.A., 2000. Gravity in a lattice Boltzmann model. Physical Review E, 61(5), p.5307.
Cengel Y.A., Boles M.A., 2002. Thermodynamics: an engineering approach. Sea.
Chen, L., Kang, Q., Mu, Y., He, Y.L. and Tao, W.Q., 2014. A critical review of the pseudopotential multiphase lattice Boltzmann model: Methods and applications. International journal of heat and mass transfer, 76, pp.210-236.
Chen, S. and Doolen, G.D., 1998: "Lattice Boltzmann method for fluid flows", Annual review of fluid mechanics, 30(1), pp.329-364.
Gunstensen AK, Rothman DH, Zaleski S, Zanetti G. 1991. Lattice Boltzmann model of immiscible fluids. Phys. Rev. A. 43:4320 – 27.
Guo, Z., Zheng, C. and Shi, B., 2002. Discrete lattice effects on the forcing term in the lattice Boltzmann method. Physical Review E, 65(4), p.046308.
Hussein M.A., 2010: "On the theoretical and numerical development of Lattice Boltzmann models for biotechnology and its applications", PhD. Technische Universität München, München.
Koelman, J.M.V.A., 1991: "A simple lattice Boltzmann scheme for Navier-Stokes fluid flow", EPL (Europhysics Letters) 15(6): p.603.
Krüger, T., Kusumaatmaja, H., Kuzmin, A., Shardt, O., Silva, G. and Viggen, E.M., 2017. The Lattice Boltzmann Method. Springer.
Ladd, A.J.C. and Verberg, R., 2001. Lattice-Boltzmann simulations of particle-fluid suspensions. Journal of Statistical Physics, 104(5-6), pp.1191-1251.
Mobarak M., **2018**: "Lattice Boltzmann Method for Flow Analysis in Subsonic Axial Compressor", M.Sc. Thesis - Cairo University.
Shan, X. and Chen, H., 1993. Lattice Boltzmann model for simulating flows with multiple phases and components. *Physical Review E*, *47*(3), p.1815.
Shan, X. and Chen, H., 1994. Simulation of nonideal gases and liquid-gas phase transitions by the lattice Boltzmann equation. Physical Review E, 49(4), p.2941.
Succi, S., 2001: "The lattice Boltzmann equation: for fluid dynamics and beyond", Oxford university press.
Swift MR, Osborn WR, Yeomans JM. 1995. Lattice Boltzmann simulation of nonideal fluids. Phys. Rev. Lett. 75:830–33
Swift MR, Orlandini SE, Osborn WR, Yeomans JM. 1996. Lattice Boltzmann simulations of liquid-gas and binary-fluid systems. Phys. Rev. E 54:5041–52
Yuan, P. and Schaefer, L., 2006. Equations of state in a lattice Boltzmann model. Physics of Fluids, 18(4), p.042101.
Yu, Z. and Fan, L.S., 2010. Multirelaxation-time interaction-potential-based lattice Boltzmann model for two-phase flow. *Physical Review E*, *82*(4), p.046708.

GALA e.V., Karlsruhe, Germany, ISBN 978-3-9816764-6-4